Nevada Seismological Laboratory Rapid Seismic Monitoring Deployment and Data Availability for the 2020 M_{ww} 6.5 Monte Cristo Range, Nevada, Earthquake Sequence

Jayne M. Bormann*1, Emily A. Morton1, Kenneth D. Smith1, Graham M. Kent1, William S. Honjas1, Gabriel L. Plank¹, and Mark C. Williams¹

Abstract

The Nevada Seismological Laboratory (NSL) at the University of Nevada, Reno, installed eight temporary seismic stations following the 15 May 2020 $M_{\rm ww}$ 6.5 Monte Cristo Range earthquake. The mainshock and resulting aftershock sequence occurred in an unpopulated and sparsely instrumented region of the Mina deflection in the central Walker Lane, approximately 55 km west of Tonopah, Nevada. The temporary stations supplement NSL's permanent seismic network, providing azimuthal coverage and nearfield recording of the aftershock sequence beginning 1-3 days after the mainshock. We expect the deployment to remain in the field until May 2021. NSL initially attempted to acquire the Monte Cristo Range deployment data in real time via cellular telemetry; however, unreliable cellular coverage forced NSL to convert to microwave telemetry within the first week of the sequence to achieve continuous real-time acquisition. Through 31 August 2020, the temporary deployment has captured near-field records of three aftershocks $M_{\rm L} \ge 5$ and 25 $M_{\rm L}$ 4-4.9 events. Here, we present details regarding the Monte Cristo Range deployment, instrumentation, and waveform availability. We combine this information with waveform availability and data access details from NSL's permanent seismic network and partner regional seismic networks to create a comprehensive summary of Monte Cristo Range sequence data. NSL's Monte Cristo Range temporary and permanent station waveform data are available in near-real time via the Incorporated Research Institutions for Seismology Data Management Center. Derived earthquake products, including NSL's earthquake catalog and phase picks, are available via the Advanced National Seismic System Comprehensive Earthquake Catalog. The temporary deployment improved catalog completeness and location quality for the Monte Cristo Range sequence. We expect these data to be useful for continued study of the Monte Cristo Range sequence and constraining crustal and seismogenic properties of the Mina deflection and central Walker Lane.

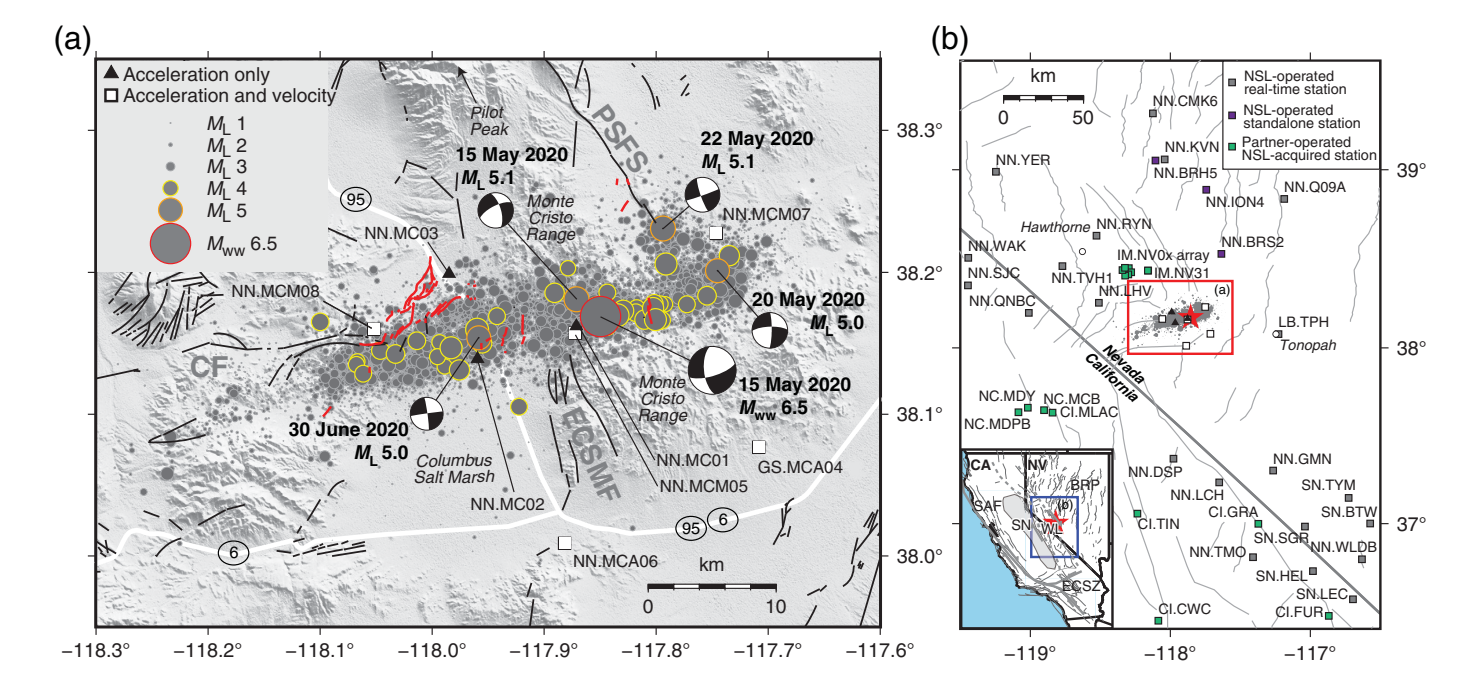
Cite this article as Bormann, J. M., E. A. Morton, K. D. Smith, G. M. Kent, W. S. Honjas, G. L. Plank, and M. C. Williams (2021). Nevada Seismological Laboratory Rapid Seismic Monitoring Deployment and Data Availability for the 2020 $M_{\rm ww}$ 6.5 Monte Cristo Range, Nevada, Earthquake Sequence, Seismol. Res. Lett. 92, 810-822, doi: 10.1785/0220200344.

Introduction

The 15 May 2020 [11:03:27 UTC; 04:03:27 Pacific Daylight Time (PDT)] Mww 6.5 Monte Cristo Range, Nevada, earthquake and aftershock sequence occurred in an unpopulated and sparsely instrumented region of the Mina deflection in the central Walker Lane (Fig. 1), approximately 55 km west-northwest of Tonopah, Nevada. This was the largest earthquake to occur in Nevada since the 16 December 1954 M 7.1 Fairview Peak and M 6.9 Dixie Valley sequence. The sequence falls within the Nevada Seismological Laboratory (NSL) permanent seismic network footprint and the U.S. Geological Survey (USGS) Advanced National Seismic System (ANSS) Nevada reporting region. NSL and partner networks recorded the $M_{\rm ww}$ 6.5 mainshock at 42 seismic stations within 200 km of the epicenter (Fig. 2); however, only two three-component stations within 70 km of the epicenter were

^{1.} Nevada Seismological Laboratory, University of Nevada, Reno, Nevada, U.S.A. *Corresponding author: jbormann@unr.edu

[©] Seismological Society of America



operating with real-time telemetry during the events: IM.NV31 (39.1 km) and NN.LHV (56.5 km).

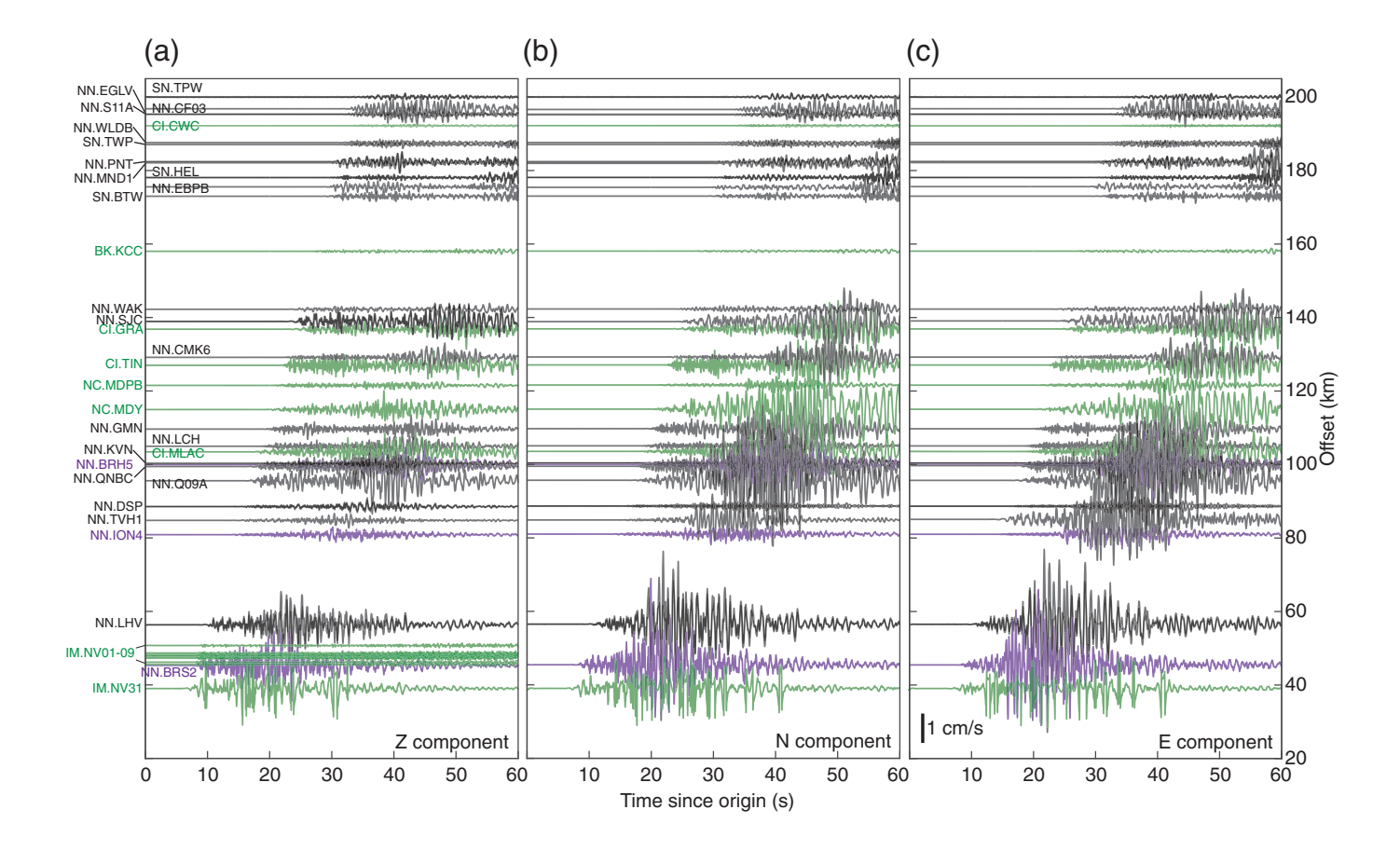
To increase the station density in the near-field rupture region and fill gaps in azimuthal coverage, NSL initialized a temporary aftershock monitoring deployment. In total, eight seismic stations were installed around the Monte Cristo Range rupture between 16 and 18 May 2020 (locations shown in Fig. 1). The remote location of the Monte Cristo Range sequence limited the use of cellular telemetry to achieve continuous real-time data acquisition to only three stations. The remaining five stations operated in stand-alone mode until NSL technicians converted the deployment to real-time telemetry on NSL's private microwave network between 21 and 24 May 2020.

Rapid temporary seismic monitoring deployments following large earthquakes present opportunities to capture critical perishable seismological data. Near-field observational records allow detailed study of earthquake source properties, fault structure and sequence evolution, seismic-wave propagation and tomography, and strong ground motion (as summarized by Cochran *et al.*, 2020). Furthermore, aftershock sequences provide our highest likelihood opportunities to record near-field ground-motion records from moderate to large earthquakes (Cochran *et al.*, 2020).

The $M_{\rm ww}$ 6.5 Monte Cristo Range mainshock ruptured a 35 km long, east–northeast-striking section of a previously unrecognized eastward extension of the left-lateral Candelaria fault, with aftershocks extending onto the eastern Columbus Salt Marsh fault and the southern extension of the Petrified Springs fault (Fig. 1; C. J. Ruhl *et al.*, unpublished manuscript, see Data and Resources). Real-time data acquisition was particularly important in monitoring the evolution and potential migration of the Monte Cristo Range sequence due to the high

Figure 1. Monte Cristo Range earthquake sequence map. (a) Sequence map showing the location of the $M_{\rm ww}$ 6.5 mainshock and 13,000+ aftershocks (gray circles with size scaled by magnitude), surface rupture associated with the $M_{\rm ww}$ 6.5 mainshock (red lines, Dee et al., 2020; Koehler et al., 2021), regional faults from the U.S. Geological Survey (USGS) Quaternary Fault and Fold Database (black lines, USGS, 2020), and locations of the portable deployment (black triangles, threechannel strong-motion stations; white squares, six-channel broadband and strong-motion stations). Moment tensors for the mainshock and M_1 5+ aftershocks are shown and labeled with event day and magnitude. Faults associated with the rupture include the Candelaria fault (CF), the eastern Columbus Salt Marsh fault (ECSMF), and the southern extension of the Petrified Springs fault system (PSFS). White lines show major highways US 95 and US 6. (b) Regional map showing the locations of permanent digital seismic stations (colored squares) active during the Monte Cristo Range mainshock (red star) and aftershock sequence (gray dots). Portable deployment stations are shown using black triangles and white squares as in panel (a). Nearby towns of Tonopah and Hawthorne, Nevada, shown with white circles. Thin gray lines show fault sources from the 2014 National Seismic Hazard Model (Shumway, 2019), and the red box marks the extent of panel (a). Inset map shows the Monte Cristo Range sequence mainshock (red star) in relation to elements of the Pacific-North American plate boundary in Nevada (NV) and California (CA). Blue box marks the extent of panel (b). BRP, Basin and Range Province; ECSZ, Eastern California Shear Zone; NSL, Nevada Seismological Laboratory; SAF, San Andreas fault; SN, Sierra Nevada block; WL, Walker Lane.

aftershock productivity and slow decay of the sequence $(p = 0.8, C. J. Ruhl \ et \ al.$, unpublished manuscript, see Data and Resources), a pattern that is typical of past Walker Lane earthquake sequences and swarms (C. J. Ruhl $et \ al.$, unpublished manuscript, see Data and Resources).



Here, we describe the temporary deployment details and present seismic data from the Monte Cristo Range sequence recorded by NSL at the University of Nevada, Reno (UNR) and collaborating partner networks, including BK, CI, GS, IM, LB, and NC (Table 1). The dataset covers the $M_{\rm ww}$ 6.5 mainshock and >13,000 aftershocks. These data are the basis for NSL earthquake products, such as phase picks, hypocenters, magnitudes, focal mechanisms, moment tensors, and ShakeMaps, submitted to the USGS ANSS Comprehensive Earthquake Catalog (ComCat, see Data and Resources, for details). We present the magnitude versus time progression of the aftershock sequence, which demonstrates the utility of rapid temporary aftershock deployments in increasing catalog completeness, and seismic records from an $M_{\rm L}$ 5.09 aftershock recorded on the portable array. Data from the temporary stations provide better control on absolute event locations, relative relocations allowing for detailed imaging of Monte Cristo Range rupture subsurface fault geometry and source characterization (C. J. Ruhl et al., unpublished manuscript, see Data and Resources), geodetic studies of the Monte Cristo Range sequence (Hammond et al., 2020), and ground-motion studies. We expect these data to be useful to the broader seismological community in continued study of the Monte Cristo Range sequence, constraining crustal properties of the Mina deflection and central Walker Lane, and expanding understanding of earthquake source processes.

Figure 2. Velocity record section of the mainshock. Waveforms of (a) vertical, (b) north, and east (c) components that recorded the $M_{\rm ww}$ 6.5 mainshock, plotted by site distance. Sites acquired and maintained by NSL (network codes NN and SN) are colored black, and sites from partner networks are colored green (network codes IM, CI, BK, NC). Purple waveforms are stand-alone sites without telemetry operated by NSL. Data from these sites were recovered two months after the mainshock. Waveforms are highpass filtered at 1 Hz. Vertical line at the bottom left of the east component panel denotes 1 cm/s of corresponding ground motion.

NSL Seismic Monitoring and Data Products

NSL currently operates 114 permanent digital seismic stations in Nevada and eastern California with publicly available continuous data under the NN and SN network codes through a cooperative agreement with the USGS. We import real-time feeds from collaborating networks (BK, CI, IM, NC, WR, UU, and UW) to assist in azimuthal coverage for local earthquake locations within our network footprint. NSL acquires data in real time from most ANSS-supported seismic sites via NSL's private, high-speed microwave network, supplemented by cellular telemetry outside the microwave network footprint. In addition, NSL operates 72 stations in support of projects on the Nevada National Security Site (NNSS)

TABLE 1

Seismic Network Operators and Network Codes in the Monte Cristo Range Area

Network Code	Network	Status	Operator
NN	Nevada Seismic Network	Permanent and portable	Nevada Seismological Laboratory, UNR
SN	Southern Nevada Seismic Network	Permanent	Nevada Seismological Laboratory, UNR
LB	Leo Brady (Nevada sites)	Permanent	Nevada Seismological Laboratory, UNR and MSTS
ВК	Berkeley Digital Seismic Network	Permanent	Berkeley Seismological Laboratory, UCB
CI	Southern California Seismic Network	Permanent	Caltech and USGS Pasadena
GS	U.S. Geological Survey Networks	Portable	USGS Albuquerque Seismological Laboratory
IM	NVAR Array	Permanent	Southern Methodist University
NC	Northern California Seismic Network	Permanent	USGS Menlo Park

Caltech, California Institute of Technology; MSTS, Mission Support and Test Services, contractor for the Nevada National Security Site; NVAR, Nevada Seismic Array; UCB, University of California, Berkeley; UNR, University of Nevada, Reno; USGS, U.S. Geological Survey.

and seven stations funded by the Barrick and Newmont Goldcorp mining operations (now operating as the Nevada Gold Mines). Waveform data from these stations are restricted; however, the stations are used in the development of NSL earthquake products, and phase picks are sent to ComCat.

NSL operates seismic stations with a variety of sensor types. Stations are classified as (1) three-component broadband stations, which generally also include three-component strongmotion sensors; (2) three-component short-period digital stations; and (3) three-component strong-motion stations, which may have an additional vertical-only short-period sensor. ANSS-supported station coverage is concentrated in highstrain areas along the Nevada-California border and near the Reno-Carson City and Las Vegas urban areas. Between May 2019 and May 2020, NSL stopped acquisition from most remaining analog stations in eastern California and western Nevada. Digital upgrades of analog stations are currently in progress, with work supported through ANSS-deferred maintenance opportunities and the build-out of the USGS ShakeAlert earthquake early warning system (see Data and Resources). NNSS stations greatly increase monitoring density in southern Nevada, and the seven-station Nevada Gold Mines network supplements ANSS-supported monitoring in sparsely instrumented northeastern Nevada. Broadband and shortperiod waveforms for ANSS-supported stations are acquired at 100 samples per second, and most strong-motion waveforms are acquired at 200 samples per second.

NSL uses the Boulder Real Time Technologies Antelope environmental monitoring software for real-time data acquisition and earthquake processing (see Data and Resources). Earthquake arrivals are automatically detected and associated, and the corresponding events are located by the Antelope system. Antelope identifies automatically detected events with a root mean square travel-time residual of <1.5 s as earthquakes, and they are saved in NSL's local database.

Automatically detected and located earthquakes with Richter magnitudes $M_{\rm L} > -0.5$ are published to ComCat in real time using the USGS Product Distribution Layer (PDL) platform (see Data and Resources). We impose an additional criterion that earthquakes with $M_L > 3.0$ must have at least five phases for automatic ComCat submission; however, we temporarily disabled the phase criterion at the onset of the Monte Cristo Range sequence due to the sparse station coverage prior to the portable deployment. NSL seismic analysts review and manually relocate all automatically detected events and identify and locate earthquakes missed by the automatic detection system daily; additional events and revised locations are subsequently updated in ComCat via PDL. Over the 5 yr prior to the Monte Cristo Range sequence, NSL contributed an average of 13,500 earthquakes per year to ComCat (Table 2), with between 98.3% and 99.9% of annual events seismologist reviewed.

NSL provides the following waveform and earthquake products for use by the seismological community:

- Continuous waveforms and station metadata under network codes NN and SN via the Incorporated Research Institutions for Seismology (IRIS) Data Management Center (DMC).
- 2. Earthquake catalog with automatic and seismologist-reviewed origin times, hypocenters, and local Richter magnitudes $(M_{\rm L})$ via ComCat.
- 3. Associated phase arrival times picks via ComCat.
- 4. ShakeMaps for $M_{\rm w} \ge 3.2$ via ComCat (in progress of transitioning production to National Earthquake Information Center).
- 5. Seismologist-reviewed focal mechanisms for most events $M_{\rm L} \ge 2$ via ComCat.
- 6. Seismologist-reviewed moment tensors for most events $M_{\rm L} \ge 3.5$ created using the MTINV program (Ichinose *et al.*, 2003) via ComCat.

TABLE 2 Monte Cristo Range Sequence Compared to Previous 5 Yr of Nevada Seismological Laboratory (NSL) Earthquake **Products**

	Year 1	Year 2	Year 3	Year 4	Year 5	Monte Cristo Range Sequence	
NSL Earthquake Products	February 2015–January 2016	February 2016–January 2017	February 2017–January 2018	February 2018–January 2019	February 2019–January 2020	15 May 2020–31 August 2020	
Total events	15,621	17,829	15,362	11,785	8,672	13,954	
% Events reviewed	99.8%	99.9%	99.8%	99.7%	98.3%	N/A*	
N $(M_L \ge 2.0)$	1,151	676	440	449	488	2,463	
$N (M_L \ge 3.0)$	171	107	50	35	61	381	
N $(M_L \ge 4.0)$	21	13	5	1	11	46	
N $(M_L \ge 5.0)$	1	3	0	0	1 [†]	5	
$N (M_L \ge 6.0)$	0	0	0	0	1 [†]	1	
Focal mechanisms	73	308	326	273	76	4 [‡]	
Moment tensors	80	41	25	11	13	18	
ShakeMaps	79	54	24	10	14	268	

^{*}NSL analysts are currently reviewing events in the MCR sequence. NSL plans to review all MCR events $M_L \ge 2$, although we anticipate it will take many months after sequence productivity slows.

Portable Deployment

Immediately following the 15 May 2020 mainshock, NSL began planning for a rapid three-station strong-motion deployment. NSL technicians prepared the portable kits and mobilized from the UNR campus to the field the afternoon of 15 May 2020, with deployment planned for 16 May 2020. Concurrent with NSL mobilization, the USGS Albuquerque Seismological Laboratory (Albuquerque, New Mexico) and Earthquake Science Center (Menlo Park, California) shipped a total of five portable six-channel broadband and strong-motion kits to the UNR campus. The USGS units arrived at NSL between the evening of 15 May 2020 and the morning of 16 May 2020, and a second NSL team mobilized to the field with these kits in the late afternoon of 16 May 2020. Travel restrictions relating to the ongoing COVID-19 pandemic prevented USGS personnel from assisting with the deployment, and all stations were installed by NSL field teams with remote support provided by the USGS Albuquerque Seismological Laboratory. In total, NSL deployed eight temporary stations within 15 km of the hypocenter and aftershock zone between 16 and 18 May 2020 (Fig. 1). Surface rupture was discovered subsequent to the installation of the temporary stations and is mainly located in the western half of the aftershock region (Koehler et al., 2021). Stations are expected to remain in the field for approximately 1 yr (until May 2021).

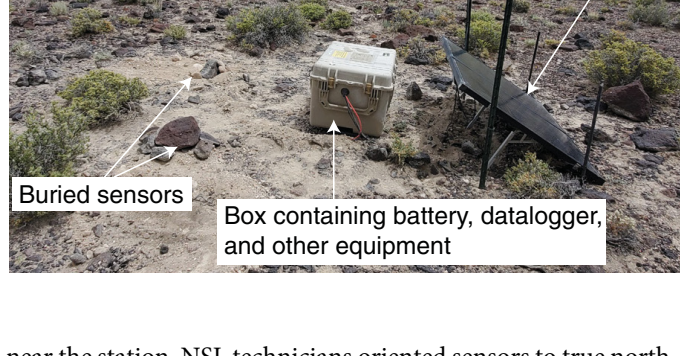
Monte Cristo Range sequence temporary stations fall into two station class types: NSL-built strong-motion stations and USGS-built six-channel broadband and strong-motion stations (Fig. 3). The NSL-built stations (Fig. 3a,b) use a Kinemetrics Etna2 integrated strong-motion (accelerometer) sensor and datalogger secured to a buried concrete paver block. The sensor and paver are covered with a bucket and subsequently buried underground. The NSL-built stations are powered by two 6 V 224 Ah batteries connected in series and solar panels. Batteries, supporting electronics, communication equipment, and Global Positioning System (GPS) antennas are stored in a large box above ground or mounted to poles near the station. The USGS-built six-channel stations (Fig. 3c,d) use the USGS traditional temporary free-field deployment kits (as described in Cochran et al., 2020). These stations include Nanometrics Trillium Compact broadband (velocity) and Kinemetrics EpiSensor strong-motion (accelerometer) sensors that are buried underground with REF TEK 130 (RT-130) dataloggers. Kits provided by the USGS Menlo Park Earthquake Science Center are powered by one 12 V 60 Ah battery and solar panel, and kits provided by USGS Albuquerque Seismological Laboratory are powered by NSL-supplied two 6 V 224 Ah batteries and solar panels. Dataloggers, batteries, supporting electronics, GPS antennas, and communications equipment are stored in a large box above ground or mounted to poles

[†]Ridgecrest **M** 6.4 event outside of NSL authoritative region, but adjacent to NSL eastern California network coverage.

^{*}NSL focal mechanisms are produced manually by analysts. Monte Cristo Range sequence productivity has limited these efforts.

(a) (b) Radio and microwave antenna Box containing battery, charge controller, modem, Buried Etna2 mounted on **Bucket covering** and other equipment accelerometer burried concrete block buried Etna2 (d) (c)

Solar panel





near the station. NSL technicians oriented sensors to true north using a handheld compass. Table 3 provides Monte Cristo Range temporary station information including station names, acquiring network, datalogger and sensor types, sample rates, and recording method. Broadband (velocity) channels are recorded at 100 samples per second, and strong-motion (accelerometer) channels are recorded at 200 samples per second.

Installing temporary stations with real-time telemetry following the 15 May 2020 mainshock was a particularly important and challenging aspect of NSL's response because of the remote location and sparse permanent station density surrounding the sequence. We initially planned to install all eight portable stations with real-time cellular telemetry to reduce uncertainty in aftershock locations and monitor potential sequence migration; however, when NSL field teams arrived at the aftershock zone on the evening of 15 May 2020, there was no cellular coverage in the Columbus Salt Marsh, nor between U.S. Highway 95 and the Monte Cristo Range. NSL technicians built a cellular-telemetered microwave access point southeast of the intersection of U.S. Highway 95 and U.S. Highway 6 to provide line of sight microwave telemetry for NSL-built strong-motion portable station MC02, the first

Figure 3. Photos of temporary station installations. (a) NSL-built accelerometer portable installation at MC02 showing location of buried sensor, box containing the battery, charge controller, modem, and supporting equipment, solar panel, and microwave radio and antenna. (b) Etna2 deployment strategy. The Etna2 sensor is mounted and leveled on a buried concrete block (left), and a 5 gal bucket covers the sensor and block before burial of the sensor (right). (c) USGS six-channel broadband and accelerometer installation at MCM07 showing location of buried sensors; box containing the datalogger, battery, modem, and supporting equipment; solar panel; and microwave radio and antenna. (d) Images showing partially buried Trillium Compact broadband sensor (left) and accelerometer (right) in Hutt vaults.

temporary station, online 16 May 2020 at 04:00:00 PDT (11:00 UTC). Cellular coverage returned to the sequence region 16 May 2020 around 8:30 a.m. PDT (15:30 UTC), and NSL crews installed two additional strong-motion stations on cellular telemetry (MC01 and MC03). The working hypothesis was that a cellular tower must have gone down during the earthquake, and that service had been restored. Unfortunately, cellular service continued to be intermittent, with service

TABLE 3
Portable Deployment Station Information

Station Type	Network	Station	Datalogger	Recording	Sensor	Location	Channels	Sample Rate (Samples per Second)	Stream Type
Real-time strong-motion only	NN	MC01 MC02 MC03	Etna2	Real-time microwave	Etna2 (EpiSensor ES-Deck)		HN [ENZ]	200	Continuous
Real-time six channel	NN	MCA06 MCM05 MCM07 MCM08	RT-130	On-site and real-time microwave	Trillium Compact		HH [ENZ]	100	Continuous
					EpiSensor		HN [ENZ]	200	Continuous
	GS	MCA04	RT-130	On-site and real-time cellular	Trillium Compact	00	HH [12Z] LH [12Z]	100	Continuous Continuous
					EpiSensor	20	HN [12Z]	200	Triggered
							LN [12Z]	1	Continuous

for only 4–8 hr/day (see data availability chart in Fig. 4). In consultation with the USGS Albuquerque Seismological Laboratory, two of the USGS portable kits were deployed on cellular telemetry (MCA04 with reliable service from a tower near Tonopah, Nevada, and MCA06 on a microwave link to the NSL cellular access point), and the remaining three stations (MCM05, MCM07, and MCM08) were temporarily deployed in stand-alone mode until a reliable real-time telemetry could be established.

Because of the high productivity and slow decay of this aftershock sequence, continued operation of the portable array in stand-alone mode with intermittent cellular coverage was not a desirable monitoring strategy. NSL technicians returned to the field 21–24 May 2020 to complete an analog-to-digital point to multipoint conversion at the existing NSL telemetry relay at Pilot Peak (Fig. 1), north of the sequence, which had line of sight to the deployment. The field teams converted the portable stations from cellular or stand-alone mode to digital microwave telemetry, leaving only MCA04, which is acquired by the GS network, on cellular telemetry (Fig 4).

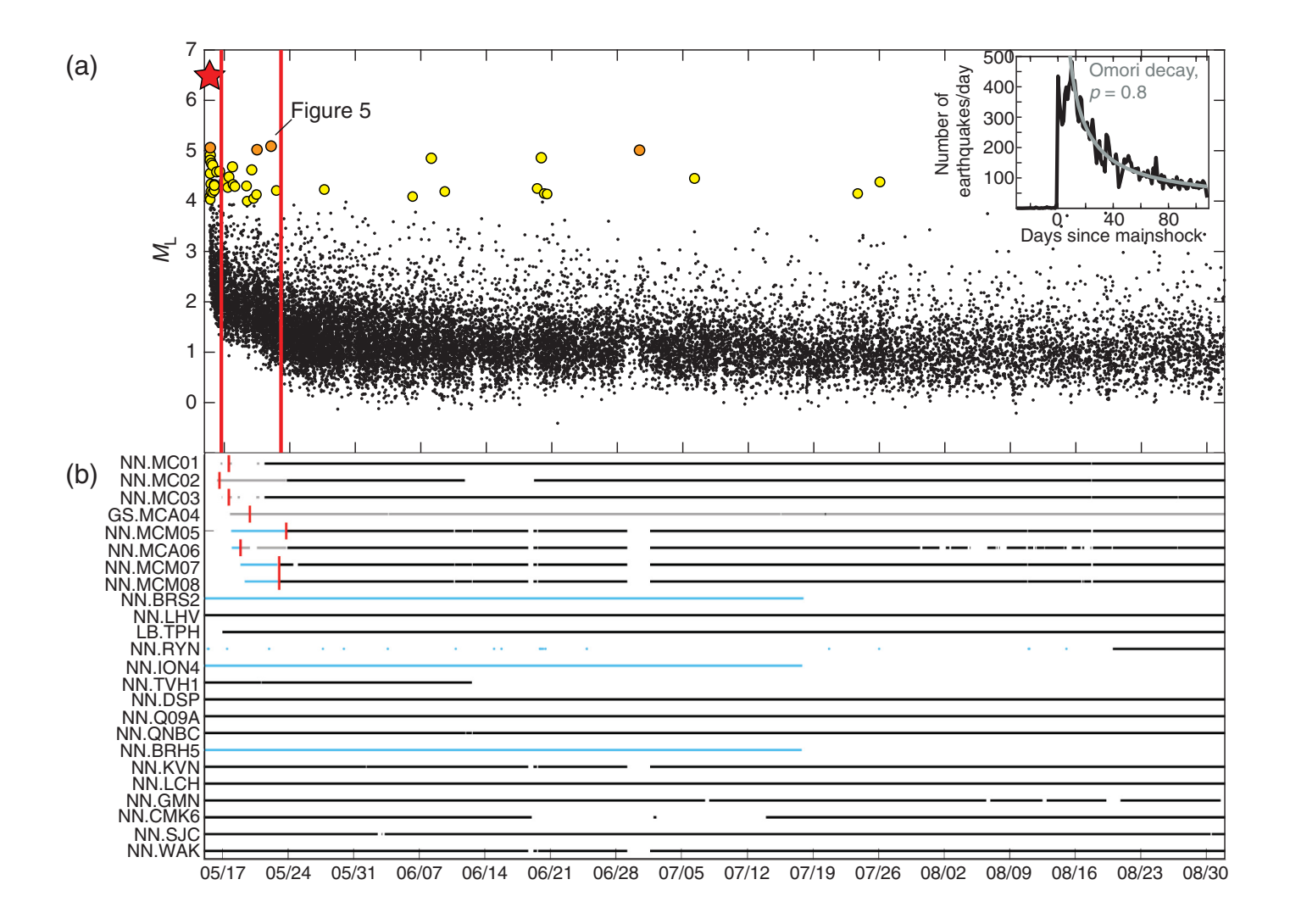
Sequence Data Availability

In addition to the eight temporary-station deployment, NSL operates 13 permanent digital seismic stations with real-time telemetry within 150 km of the Monte Cristo Range mainshock. Eleven of these stations were operating at the time of the mainshock (Fig. 2), and the two other stations were repaired or upgraded during the sequence (Fig. 4b). NN.LHV was the closest NSL permanent station to the mainshock epicenter at 56 km distance. NSL imports seismic data from the IM network

Nevada Array sites NV08, NV09, and NV31 for routine monitoring (NV-array operated by Southern Methodist University, Table 1), and these stations provided the closest real-time mainshock records at distances between 39 and 51 km (Figs. 1 and 2). Immediately following the 15 May 2020 mainshock, we added additional IM sites (NV01–NV07) to our data import to aid in sequence locations. Seismic stations with continuous waveform data from the sequence are shown in Figure 1b, with partner network information summarized in Table 1.

To increase sequence coverage, NSL repaired and completed communication upgrades at nearby NSL-operated sites LB.TPH and NN.RYN. On 16 May 2020, NSL technicians repaired the power system and restored real-time acquisition at site LB.TPH, jointly operated by NSL and Mission Support and Test Services (MSTS) in Tonopah, Nevada, approximately 57 km from the mainshock epicenter. This repair resulted in additional near-field observations and improved azimuthal coverage (Figs. 1 and 4b). Site NN.RYN is located approximately 77 km from the mainshock epicenter (Fig. 1). It was operated in triggered stand-alone mode during much of the beginning of the sequence due to pending communication upgrades. NN.RYN recorded the mainshock, but only the largest aftershocks triggered recording at the site. The NN.RYN real-time communication upgrade was completed on 20 August 2020, restoring continuous waveform acquisition and archival (Fig. 4b).

In addition to ANSS-supported seismic monitoring, NSL operates permanent seismic stations NN.BRS2, NN.ION4, NN.BRH5, and NN.CMK6, located to the northeast of the Monte Cristo Range sequence, in support of NNSS research programs. Continuous waveform data from NN.CMK6 are



acquired in real time, used in NSL routine analysis, and publicly available via the IRIS DMC. NN.BRS2, NN.ION4, and NN.BRH5 are restricted sites operated in stand-alone mode, with event data from NNSS experiments released for public use after a hold period. On 17–18 July 2020, we recovered the data from these sites for use in aftershock location and to refine the mainshock location due to their proximity and azimuthal coverage relative to the source region (Figs. 1 and 2). MSTS, contractor for NNSS research programs, has given NSL permission to release continuous waveform data from stations NN.BRS2, NN.ION4, and NN.BRH5 recorded between 15 May and 18 July 2020 to the public via the IRIS DMC for research purposes (Fig. 4b).

Waveform availability from NSL-operated permanent and temporary stations located within 150 km of the mainshock is summarized in Figure 4b. The 13 NSL permanent stations have an average of 84.26% data availability from the time of the mainshock through 31 August 2020, and seven of these sites have >99% data availability. The temporary deployment stations all have >90% data availability from the time of their installation (16–18 May 2020) through 31 August 2020, averaging 93% data availability (Fig. 4b).

Figure 4. Earthquakes and waveform availability with time (mmdd). (a) Seismicity by local magnitude (black); earthquakes with $M_1 \ge 4$ are colored yellow, earthquakes $M_1 \ge 5$ are colored orange, and the $M_{\rm ww}$ 6.5 mainshock is the red star. (b) Waveform availability for the temporary Monte Cristo Range sequence and NSL-operated permanent stations within 150 km of the mainshock. Solid lines represent times with seismic data archived and available via Incorporated Research Institutions for Seismology Data Management Center. Gray lines indicate times when the eight temporary sites were telemetered via cellular communications rather than NSL's private microwave network. Blue lines indicate times when sites were operating in stand-alone mode (i.e., not telemetered in real time), and the data were manually recovered from the field. Red lines in panels (a,b) correspond to the times the temporary sites were incorporated into NSL real-time operations; in panel (a), they reflect the time of the first and last site incorporations. The inset in panel (a) represents number of earthquakes per day with Omori aftershock decay fit. Best-fitting aftershock decay corresponds to a decay parameter p = 0.8.

The largest data gaps from the temporary deployment occur on MC02 (11 June 2020 20:19:25 UTC-19 June 2020 06:36:02 UTC), sites MCM05, MCA06, MCM07, and MCM08 (18 June

2020 15:33:46 UTC-19 June 2020 03:53:23 UTC and 29 June 2020 05:13:21 UTC-1 July 2020 15:21:06 UTC), and periodically on-site MCA06 (Fig. 4b). MC02 uses an Etna2 integrated sensor and datalogger with real-time streaming via an Antelope-compatible object ring buffer (ORB). The datalogger to Antelope ORB-to-ORB process failed on 11 June 2020. We remotely restarted the local MC02 ORB on 19 June 2020, and the issue has not recurred. Sites MCM05, MCA06, MCM07, and MCM08 use RT-130 dataloggers. The corresponding 18-19 June 2020 and 29 June-1 July 2020 data gaps occurred when NSL's REF TEK acquisition system had stalled. This problem affected real-time acquisition for all NSL-operated stations with RT-130 dataloggers (e.g., NN.KVN and NN.WAK, Fig. 4b), resulting in corresponding apparent decreases in Monte Cristo Range sequence productivity (Fig. 4a). We increased the buffer size for REF TEK acquisition, and the issue has not recurred. Site MCA06 had recurring acquisition failures for the period of 30 July-26 August 2020 due to a repeating failure of the RT-130 datalogger automatic data dump process. NSL staff were able to remotely clear datalogger random access memory and restart acquisition; however, the issue persisted. The Albuquerque Seismological Laboratory quickly provided a replacement datalogger, which was installed on 26 August 2020. The issue has not recurred since the datalogger swap.

Two issues have occurred that pertain to the data quality of site MC03 and catalog completeness for Monte Cristo Range sequence. On two occasions, the GPS lock at MC03 failed and clock quality decreased to <10% starting mid-May 2020 and again mid-June 2020. On both occasions, NSL field technicians visited the site to find the GPS cable had been severed. It is unclear if the cable damage was due to vandalism or animals. The GPS cable was replaced in both instances on 23 May 2020 and 26 August 2020, respectively. During the most recent repair, NSL technicians increased signage to deter vandalism and added a protective conduit around the GPS cable. Finally, there was a gap in NSL automatically detected and located earthquakes on 19 May 2020 18:42-21:48 UTC, causing it to appear as if no earthquakes had occurred within NSL's catalog. This resulted from a duplicate metadata entry within NSL's database, causing a detection mapping failure. The metadata duplication was rectified, and NSL analysts manually identified and located earthquakes within this time period to correct the catalog completeness.

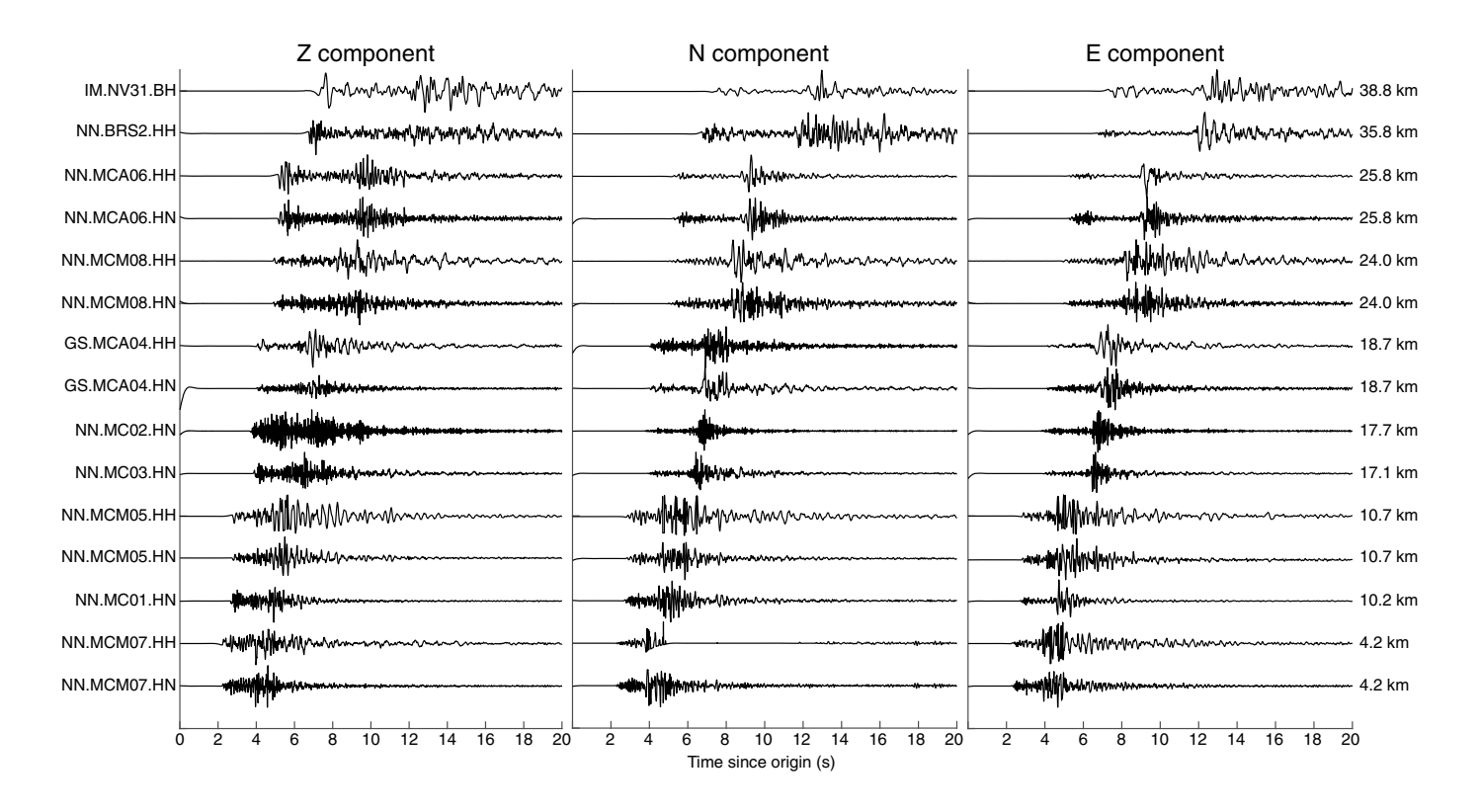
Initial Observations

NSL real-time systems have cataloged >13,000 automatically detected earthquakes in the Monte Cristo Range sequence between 15 May and 31 August 2020 (Fig. 4a and Table 2). The sequence includes 2463 events $M_{\rm L} \geq$ 2.0, outpacing Nevada statewide production from the previous 4 yr combined (Table 2). In addition, NSL has distributed 268 ShakeMaps and computed 18 moment-tensor solutions.

The Monte Cristo Range temporary deployment began on the same day as the 15 May 2020 mainshock event, with all eight stations installed between 16 and 18 May 2020 to provide much needed near field and azimuthal coverage for the aftershock sequence. Prior to the temporary deployment, there was no seismic coverage within 35 km of the sequence (Figs. 1 and 2). The detectable magnitude threshold dropped immediately upon the incorporation of the first temporary site (MC02) into NSL's realtime operations, ultimately decreasing from $M_{\rm L} > 1.2$ to $\sim M_{\rm L}$ 0 when the last station was added to the real-time detection system (Fig. 4a). Figure 4 shows that the detectable magnitude increases when data gaps exist for four or more of the temporary sites, further demonstrating the utility of the near-field array. The detection and location of these smaller ($M_L \le 1.2$) earthquakes are crucial for understanding sequence evolution and fault complexity (C. J. Ruhl et al., unpublished manuscript, see Data and Resources). In addition to lowering the magnitude detection threshold, the temporary deployment also captured important near-field ground-motion records for 3 $M_{\rm L} \ge 5.0$ and 25 $M_L \ge 4.0$ aftershocks through 31 August 2020 (Fig. 4a). Figure 5 shows a record section for the 22 May 2020 $M_{\rm L}$ 5.1 strike-slip aftershock that occurred in the northeast extent of the $M_{\rm ww}$ 6.5 rupture (see Fig. 1, for aftershock location). The event occurred at 7.2 km depth, and the nearest station was MCM07 at 4.2 km epicentral distance.

The detection signal to noise ratios for the temporary sites are approximately one to two orders of magnitude larger than those for the next closest real-time telemetered sites for earthquakes with $M_{\rm L} < 2.5$ (Fig. 6), which aids in more accurate phase identification. An Omori aftershock decay was fit to the sequence starting 10 days after the mainshock, with decay parameter p=0.8 (Fig. 4a, inset; C. J. Ruhl *et al.*, unpublished manuscript, see Data and Resources). This fit suggests that there may be more than 3700 earthquakes missing from the catalog on the first day of the sequence, an order of magnitude more than the 443 earthquakes currently cataloged. These events were likely missed due to the combination of a lack of near-field seismic stations and short-term incompleteness (Kagan, 2004), in which the frequent occurrence of large aftershocks early in the aftershock sequence temporarily obscures the detection of smaller events.

The temporary deployment also substantially improved sequence locations, as evidenced in the statistics for all analyst-reviewed and automatically located $M_{\rm L} > 2$ earthquake statistics (Fig. 7). Before the incorporation of the temporary seismic stations into NSL real-time acquisition and operations, Monte Cristo Range sequence event location errors, depth errors, and origin time errors (Fig. 7a–c, respectively) had a large range of values and some of the highest values during the sequence. Ninety percent of analyst-reviewed earthquakes before the incorporation of the temporary stations had location errors \leq 3.21 km, depth errors \leq 8.12 km, and origin time errors \leq 0.33 s. The location and depth error values show an immediate decrease after the incorporation of the temporary



stations into real-time operations, with 90% of location errors decreasing to ≤1.10 km, 90% of depth errors decreasing to \leq 1.40 km, and 90% of origin time errors decreasing to \leq 0.14 s after all temporary sites were included in real-time operations. Median errors decreased from 1.38 km before the temporary stations to 0.72 km after the addition of all eight temporary stations for earthquake locations, from 2.61 to 0.79 km for earthquake depths, and 0.16 to 0.07 s for origin times. Similarly, the location errors for automatically located, not-yet-reviewed earthquakes also improved; 90% of automatically located earthquakes $M_{\rm L} \ge 2$ had location errors ≤ 1.90 km, depth errors ≤4.55 km, and origin time errors ≤1.32 s. Following the incorporation of the temporary stations into real-time operations, 90% of automatic location errors decreased to ≤0.91 km, 90% of depth errors to ≤0.78 km, and 90% of origin time errors to ≤0.10 s. Median errors of automatic locations decreased from 1.16 to 0.60 km for earthquake locations, 1.73 to 0.33 km for earthquake depths, and 0.22 to 0.03 s for earthquake origin times. We note events are not duplicated in the reviewed and automatically located datasets used for this analysis; that is, the initial automatic locations for reviewed events are not represented in this automatically located statistics. Location and depth errors prior to the temporary deployment are higher for the analyst-reviewed set, likely because most of the predeployment earthquakes have been reviewed at the time of writing, resulting in only a small number of automatically located events during this predeployement period. The temporary stations also provided much-needed depth control for the earthquake locations (Fig. 7d). Prior to the deployments, aftershock depths ranged between 0 and 20 km; after the deployment, depths range

Figure 5. Record Section from an M_L 5.1 aftershock on 22 May 2020 00:22:00.589 UTC. The aftershock was located at 38.2309° N, 117.7939° W, at 7.16 km depth (event location and moment tensor shown in Fig. 1a). Stations are listed as NetworkCode.StationName.ChannelPrefix. Waveforms are high-pass filtered with two corners and two poles at 1 Hz and shown in normalized digital counts. Event–station offsets are listed along the right. Station GS.MCA04 uses H?1 and H?2 channel naming convention instead of N and E, respectively.

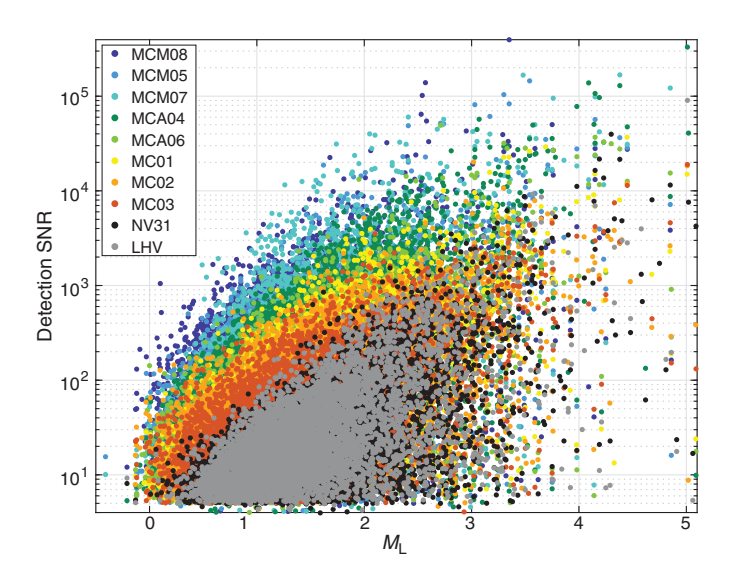
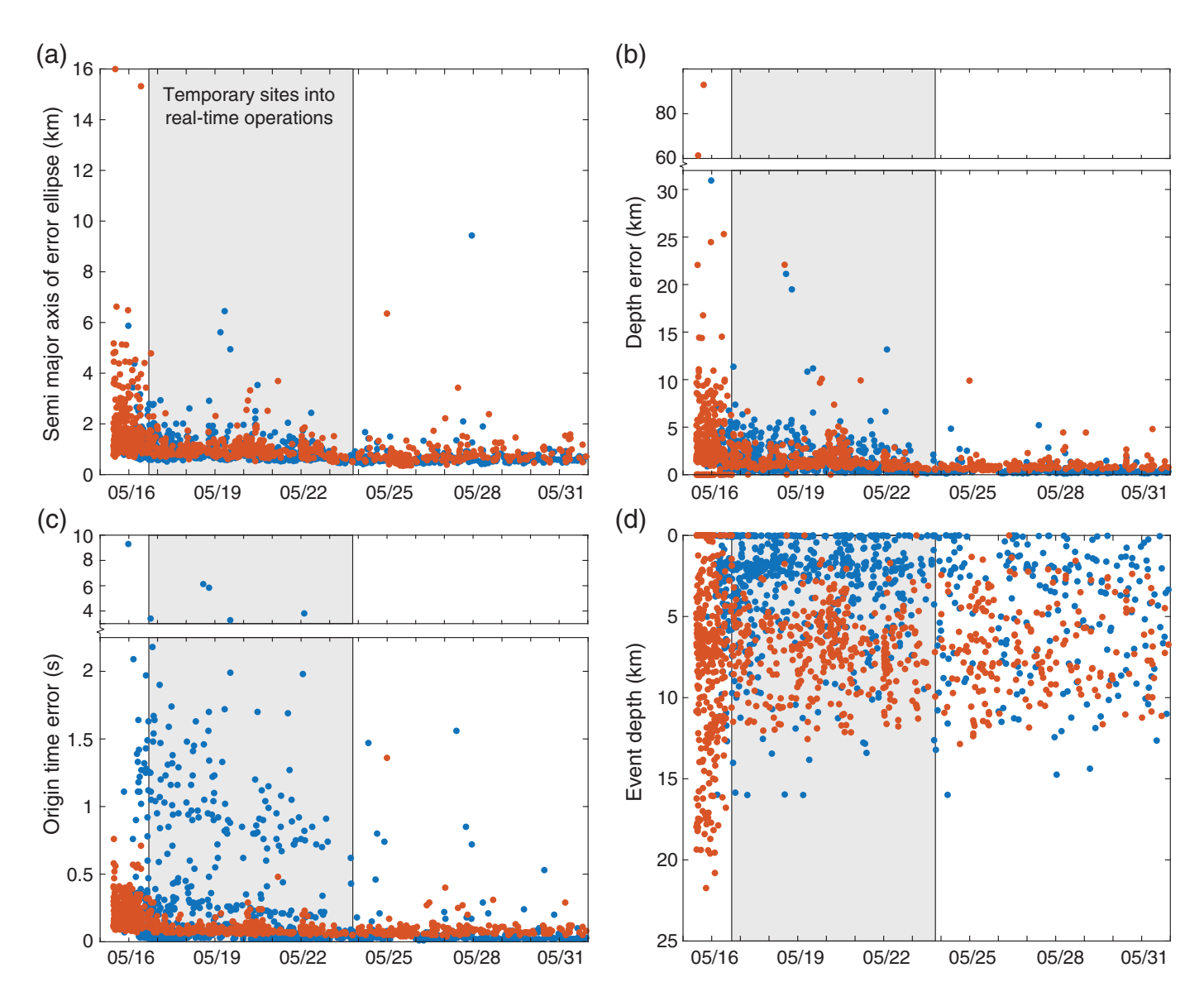


Figure 6. *P*-wave detection signal-to-noise ratio (SNR) for the eight Monte Cristo Range temporary sites and the two closest permanent, three-component, telemetered sites (NV31 and LHV) by corresponding event magnitude.



between 0 and 12 km, values typical for Walker Lane seismicity (e.g., Zuza and Cao, 2020).

Summary

The 15 May 2020 $M_{\rm ww}$ 6.5 Monte Cristo Range earthquake was the largest earthquake to occur in Nevada in more than 60 yr. In response to the event, NSL deployed eight seismic stations for rapid aftershock monitoring during 16-18 May 2020 to capture near-field records of the prolific aftershock sequence. Real-time waveform data from the temporary stations and neighboring NSL permanent stations are used in the ongoing monitoring of the sequence, and available in near-real time to the seismological community through the IRIS DMC. NSL earthquake products, including the Monte Cristo Range sequence catalog, phase picks, moment tensors, focal mechanisms, and ShakeMaps, are available through the ANSS ComCat. The Monte Cristo Range temporary deployment improved sequence monitoring as evidenced by lower magnitude detection thresholds and reduced location and depth

Figure 7. Location quality with time (mmdd) of automatically located, unreviewed earthquakes $M_L > 2$ (blue dots) and analystreviewed earthquakes (red dots). (a) Earthquake horizontal location error, (b) earthquake depth error, (c) origin time error, and (d) earthquake depth. Earthquake depths of 0 km with corresponding 0 km depth error indicate the event depth could not be constrained. Gray boxes highlight the time frame that Monte Cristo Range temporary seismic stations were incorporated into NSL's real-time operations.

spread and uncertainties. In addition, the deployment captured near-field records of more than 25 moderate magnitude M_1 4–5 aftershocks. We hope that the near-field continuous sequence waveforms and related earthquake products will be used by the seismological community for continued study of the Monte Cristo Range sequence, constraining crustal properties of the Mina deflection and central Walker Lane, and expanding our understanding of fundamental earthquake source processes.

Data and Resources

The seismic data described here were collected by the Nevada Seismological Laboratory (NSL) and U.S. Geological Survey (USGS) as a rapid response to the 15 May 2020 $M_{\rm ww}$ 6.5 Monte Cristo Range earthquake. Data from eight temporary seismic stations are archived and available in near-real time via the Incorporated Research Institutions for Seismology (IRIS) Data Management Center (DMC) at http://ds .iris.edu/ds/nodes/dmc (last accessed November 2020) under network codes NN (MC01-03, MCM05, MCA06, and MCM07-08) and GS (MCA04; DOI: 10.7914/SN/GS). Data from NSL permanent digital seismographs are also available in near-real time at the IRIS DMC under network codes NN and SN. Additional stand-alone data (stations NN.BRS2, NN.ION4, and NN.BRH5) are being made available through IRIS DMC for the time period of the Monte Cristo Range sequence. Waveform data from partner networks seismic stations are available from the following locations: CI-Southern California Seismic Network (http://www.scsn.org, last accessed November 2020; DOI: 10.7914/ SN/CI) archived at the Southern California Earthquake Data Center (https://scedc.caltech.edu, last accessed November 2020; DOI: 10.7909/ C3WD3xH1); BK—Berkeley Digital Seismic Network (http://seismo .berkeley.edu/bdsn/, last accessed November 2020; DOI: 10.7932/ BDSN) and NC-Northern California Seismic Network (http://www .ncedc.org/ncss/, last accessed November 2020) archived at the Northern California Earthquake Data Center (http://www\.ncedc.org/, last accessed November 2020; DOI: 10.7932/NCEDC); and LB-Leo Brady Network and IM-NVAR array archived at the IRIS DMC (http:// ds.iris.edu/ds/nodes/dmc, last accessed November 2020). The facilities of IRIS Data Services, specifically the Modular Utility for STAtistical kNowledge Gathering (MUSTANG) data-quality webservice, were used for data availability metrics in this article (https://service.iris.edu/ mustang/, last accessed September 2020). NSL earthquake products are generated and processed with the Boulder Real Time Technologies Antelope software (https://brtt.com/software/, last accessed November 2020), and made available through the Advanced National Seismic System (ANSS) Comprehensive Earthquake Catalog (ComCat) (https:// earthquake.usgs.gov/data/comcat/, last accessed November 2020). Earthquake locations and catalog statistics presented in Figure 1 and Table 2 were downloaded from the ANSS ComCat with origin contributor "NN-University of Nevada" (last accessed November 2020). NSL moment tensors were created using the MTINV toolkit (Ichinose et al., 2003), source code, documentation, and tutorial are available at https:// sourceforge.net/projects/mtinv/ (last accessed November 2020). Figure 1 was generated using the Generic Mapping Tools software (Wessel and Smith, 1991; Wessel et al., 2013). Data about USGS ShakeAlert earthquake early warning system are available at https://www.usgs.gov/ natural-hazards/earthquake-hazards/shakealert (last accessed November 2020). Information about USGS Product Distribution Layer platform is available at https://github.com/usgs/pdl (last accessed November 2020). Other information is from an unpublished manuscript by C. J. Ruhl, E. A. Morton, J. M. Bormann, R. Hatch-Ibarra, G. Ichinose, and K. D. Smith, Complex fault geometry of the 2020 $M_{\rm w}$ 6.5 Monte Cristo Range, Nevada earthquake sequence, submitted to Seismol. Res. Lett.

Acknowledgments

The authors are extremely grateful to the Nevada Seismological Laboratory (NSL) technicians (Alex Babb, Cameron Defabry, Patrick Hudspeth, Cory Pang, Andrew Rosenberg-Main, Charles Smart, and Kent Straley) and student field assistants (Mitch Menns, Zach Mensonides, Luke Raffaeli, and Emily Maher) for their rapid and continued response in deploying and maintaining the temporary seismic stations described in this article. The authors thank NSL seismic analysts Thomas Rennie and Mickey Cassar, and student analysts Noah Conway and Shannon Dennis for their ongoing work to review earthquakes in the very prolific aftershock sequence. The authors thank Erik Williams for administrative support throughout this entire sequence. The authors also thank Brian Shiro and an anonymous reviewer for their thoughtful reviews that improved the clarity of the article; Emily Wolin and U.S. Geological Survey (USGS) Albuquerque Seismological Laboratory team and Adria McClain and USGS Menlo Park Earthquake Science Center team for mobilizing the USGS portable kits and supporting the Monte Cristo Range aftershock deployment remotely; Rufus Catchings, Joanne Chan, and team for delivering USGS portable kits from Menlo Park to NSL; Ryan Gold (USGS event response coordinator); Cecily Wolfe (USGS Advanced National Seismic System [ANSS] coordinator); Jamie Steidl (National Strong Motion Project) for identifying and helping to rectify strong-motion metadata discrepancies; and Mission Support and Test Services (MSTS) for permission to release continuous waveform data from restricted seismic stations NN.BRS2, NN.ION4, and NN.BRH5 during the first two months of the Monte Cristo Range sequence. NSL regional seismic monitoring, earthquake product development, sequence response were funded by the USGS Cooperative Agreement Number G20AC00038 and a rapid earthquake response data collection award that supplements this agreement.

References

- Cochran, E. S., E. Wolin, D. E. McNamara, A. Yong, D. Wilson, M. Alvarez, N. van der Elst, A. McClain, and J. Steidl (2020). The U.S. Geological Survey's rapid seismic array deployment for the 2019 Ridgecrest earthquake sequence, *Seismol. Res. Lett.* 91, 1952–1960, doi: 10.1785/0220190296.
- Dee, S., R. D. Koehler, A. J. Elliott, A. E. Hatem, A. J. Pickering, I. Pierce, G. G. Seitz, C. M. Collett, T. E. Dawson, C. DeMasi, et al. (2020). Surface rupture map of the 2020 M6.5 Cristo Range earth-quake, Esmeralda and Mineral counties, Nevada, Nevada Bureau of Mines and Geology Map, scale 1:14,000.
- Hammond, W. C., G. Blewitt, C. Kreemer, R. D. Koehler, and S. Dee (2020). Geodetic observation of seismic cycles before, during and after the 2020 Monte Cristo Range earthquake using the MAGNET GPS network, Seismol. Res. Lett., doi: 10.1785/ 0220200338.
- Ichinose, G. A., J. G. Anderson, K. D. Smith, and Y. Zeng (2003). Source parameters of eastern California and western Nevada earthquakes from regional moment tensor inversion, *Bull. Seismol. Soc. Am.* **93**, 61–84.
- Kagan, Y. Y. (2004). Short-term properties of earthquake catalogs and models of earthquake source, *Bull. Seismol. Soc. Am.* **94**, 1207–1228, doi: 10.1785/012003098.
- Koehler, R. D., S. Dee, A. Elliott, A. Hatem, A. Pickering, I. Pierce, and G. Seitz (2021). Field response and surface rupture characteristics of the 2020 M 6.5 Monte Cristo Mountains earthquake, central Walker Lane, Nevada, Seismol. Res. Lett., doi: 10.1785/02202000371.

- Shumway, A. M. (2019). Data release for the 2014 National Seismic Hazard Model for the conterminous U.S., *U.S. Geol. Surv. Data Release*, doi: 10.5066/P9P77LGZ.
- U.S. Geological Survey, California Geological Survey, and Nevada Bureau of Mines and Geology (2020). Quaternary fault and fold database for the United States, available at https://www.usgs.gov/ natural-hazards/earthquake-hazards/faults (last accessed September 2020).
- Wessel, P., and W. H. F. Smith (1991). Free software helps map and display data, *Eos Trans. AGU72*, 441–446, doi: 10.1029/90EO00319.
- Wessel, P., W. H. F. Smith, R. Scharroo, J. Luis, and F. Wobbe (2013). Generic Mapping Tools: Improved version released, *Eos Trans. AGU* **94**, 409–410, doi: 10.1002/2013EO450001.
- Zuza, A. W., and W. Cao (2020). Seismogenic thickness of California: Implications for thermal structure and seismic hazard, *Tectonophysics* 782/783, 228,426, doi: 10.1016/j.tecto.2020.228426.

Manuscript received 25 September 2020 Published online 27 January 2021